Model selection for athermal cross-linked fiber networks

A. Shahsavari and R. C. Picu
Department of Mechanical, Aerospace and Nuclear Engineering, Rensselaer Polytechnic Institute, Troy, New York 12180 USA
(Received 17 January 2012; revised manuscript received 18 June 2012; published 24 July 2012)

Athermal random fiber networks are usually modeled by representing each fiber as a truss, a Euler-Bernoulli or a Timoshenko beam, and, in the case of cross-linked networks, each cross-link as a pinned, rotating, or welded joint. In this work we study the effect of these various modeling options on the dependence of the overall network stiffness on system parameters. We conclude that Timoshenko beams can be used for the entire range of density and beam stiffness parameters, while the Euler-Bernoulli model can be used only at relatively low network densities. In the high density-high bending stiffness range, strain energy is stored predominantly in the axial and shear deformation modes, while in the other extreme range of parameters, the energy is stored in the bending mode. The effect of the model size on the network stiffness is also discussed.

DOI: 10.1103/PhysRevE.86.011923 PACS number(s): 87.16.Ka, 62.20.de, 62.23.St

I. INTRODUCTION

Systems composed from fibers are ubiquitous in the living and artificial worlds. Connective tissue is composed from a mixture of fibers of different types, while the cytoskeleton of eukaryotic cells is composed from a dense network of F-actin and a sparser network of much stiffer microtubules [1]. Man-made fibers are used in a variety of consumer products such as paper, tissue and hygiene products, in protective clothing and packaging materials, to name just few applications. Fibers are used as reinforcing elements in composites of various types, ranging from common fiberglass to highly specific carbon-based materials for re-entry thermal shields of space vehicles.

Fiber networks can be classified as either thermal or athermal, depending on whether thermal fluctuations are important in their mechanics or not. Fibers large enough, with large bending stiffness, can be considered athermal [2]. For example, the F-actin fibers of the cytoskeleton are sufficiently small for thermal fluctuations to be important in their mechanics [1], while the vast majority of artificial fibers are athermal.

Given the importance of these systems, modeling of fibrous structures has become a necessity. The objectives of modeling are usually to understand the mechanisms of deformation and failure on system sub-scales, and to facilitate the design of products made from such materials [3–7]. Modeling of athermal fiber networks is usually performed by representing each fiber as a truss, i.e., an element which carries only axial loads, or a beam, which carries axial and transverse forces and bending moments. Beams can be represented either with Euler-Bernoulli (EB) or Timoshenko (T) models [7].

Several models are available for the cross-links between fibers. Specifically, one may use pin joints, which transmit no moments, rotating joints, which transmit moments only along each of the two beams crossing at given crossing point but not between them, and welded joints, which enforce that the relative angles between the crossing beams at the crossing point remain constant during deformation, and hence transmit moments along and between crossing fibers. In special applications, such as, for example, when modeling F-actin binding proteins, more complex constitutive laws can be ascribed to the cross-links [8].

An important parameter controlling the mechanics of fiber networks is the mean coordination number, z. This represents the number of fiber segments emerging from a given cross-link. It has been shown that for $z < 4$ (in 2D) a network of trusses has vanishing stiffness [9]. The role of z in controlling the mechanics of fiber networks was studied extensively [10–13]. Note that if trusses are used, all cross-links are necessarily pin joints. In most biological applications, and especially in 3D, only two fibers are in contact at each cross-link and hence the coordination number is (at most) 4 [7]. For this reason we focus here on the use of beam models for fibers and do not consider pin joints.

In this article we present a comparison of various modeling options for athermal random networks with the goal of guiding model selection. In particular, we consider EB and T beam models and welded and rotating representations for the cross-links. The quantity of interest is the overall stiffness of the network. The dependence of the network moduli (Young's, E, and shear, G) on system parameters was studied for 2D [14–17] and 3D networks [12,13,18–20]. It has been shown that the key parameters are the network density, ρ, defined as the total fiber length per unit area, and the quantity l_b, defined as the ratio of the fiber bending and axial stiffness, $l_b^2 = E_f I / E_f A$ (where I and A are the moment of inertia and the cross-sectional area of fibers, respectively). The fiber density can be expressed in terms of the fiber number density, N, and the fiber length, L_0, as $\rho = N L_0$. The findings of these works are discussed in the Results section. Here it suffices to mention that the results in all cited works [2,4,5,8–16,18–20] were obtained with the EB model and assuming either welded or rotating joints.

II. MODEL

Two-dimensional networks are generated by depositing fibers of length L_0 in a square domain of dimension L with random fiber orientation and centroid positions. Cross-links are introduced at all points where fibers intersect and for these nodes the coordination number is $z = 4$. The fiber dangling ends are eliminated as they do not store elastic energy during deformation. The cross-links at the ends of fibers have $z = 2$ or 3. Therefore, the mean coordination number takes values between 3 and 4 and varies with L_0 and ρ.

Loading is imposed by specifying displacements (a uniform far-field uniaxial, biaxial, or shear strain field) along the boundary of the domain. The results presented here are obtained

for uniaxial far-field deformation ($\varepsilon_{11} = 0; \varepsilon_{22} \neq 0; \varepsilon_{12} = 0$) imposed on a square domain. All edges are forced to remain straight during deformation and periodic boundary conditions are applied. This allows for the simultaneous determination of Young's modulus, E, and Poisson's ratio, υ.

The fiber material is considered linear elastic and fibers are characterized by their bending, axial, and effective shear stiffness, $E_f I$, $E_f A$, and $G_f A$, respectively. E_f and G_f are the fiber Young's and shear moduli, respectively. If the Timoshenko model is used [21], the total energy of the system is the sum of the strain energies associated with bending, axial, and shear deformation, i.e.,

$$U = \frac{1}{2}\sum_{\text{fibers}} \int E_f I\left(\frac{d\psi(s)}{ds}\right)^2 + E_f A\left(\frac{du(s)}{ds}\right)^2 + \lambda G_f A\left(\frac{dv(s)}{ds} - \psi(s)\right)^2 ds \quad (1)$$

In this expression, $v(s)$ represents the transverse displacement and $\frac{du(s)}{ds}$ is the axial strain at position s along the fiber. The rotation of the fiber cross-section is $\frac{dv(s)}{ds}$, while $\psi(s)$ represents the rotation of a plane that remains perpendicular to the neutral axis of the beam. Hence, $\frac{dv(s)}{ds} - \psi(s)$ represents the shear deformation of the beam. λ is a constant that is considered 0.88 (for beams with circular cross section). In the Euler-Bernoulli model [21], the last term in Eq. (1) vanishes since the model does not account for shear and, therefore, $\frac{dv(s)}{ds} = \psi(s)$. The two models give identical predictions for long, slender beams (beam length significantly larger than the cross-sectional dimensions), while the Timoshenko model gives more accurate predictions for short beams. In random fiber-networks with random orientation of fibers, the distribution function of segment lengths is Poisson [22]. Hence, a large number of short segments are present and, for given fiber diameter, one expects many segments to be too short to be properly modeled with the Euler-Bernoulli formulation. This observation motivates the present study, as we intend to establish at what system parameters the EB model ceases to provide accurate results. Conversely, we identify conditions under which the shear deformation mode should be taken into account in the energy balance of the system.

As mentioned in the Introduction, the system parameters are the fiber length, L_0, the fiber number density N, the network density $\rho = NL_0$, the mean segment length, $l_c = \pi/2\rho$ [22], and $l_b = (E_f I/E_f A)^{1/2}$ [14]. Note that for a cylindrical fiber, l_b is equal to half of the cylinder radius. The system size L can be considered as an additional parameter.

III. RESULTS

The objective of this work is to compare predictions of the effective network moduli obtained using the various models mentioned above. The moduli are expressed in terms of parameters ρ, L_0, and l_b, which are sufficient to fully define a random network of this type. Data for 96 networks with density ρ ranging from 50 to 300, fiber length L_0 ranging from 0.25 to 1, and l_b in the interval $(10^{-7}, 10^{-2})$ are presented in Fig. 1. The unit of length is selected arbitrarily. In Fig. 1(a), the Young's modulus E is normalized by $E_f A\rho$ and a constant α, which is a dimensionless quantity equal to 0.38. The variable of the horizontal axis is $w = \log_{10}[(\rho L_0)^x (l_b/L_0)^y]$. Note that since $\rho \sim l_c^{-1}$, it results that $\rho L_0 \sim L_0/l_c$. The exponents x and y are varied until the data collapse on a master curve. The two exponents x and y result: $x = 7$ and $y = 2$. The uncollapsed data for systems with $L_0 = 0.25$ and 1 are shown in Fig. 1(b), where the vertical axis is normalized by E_f.

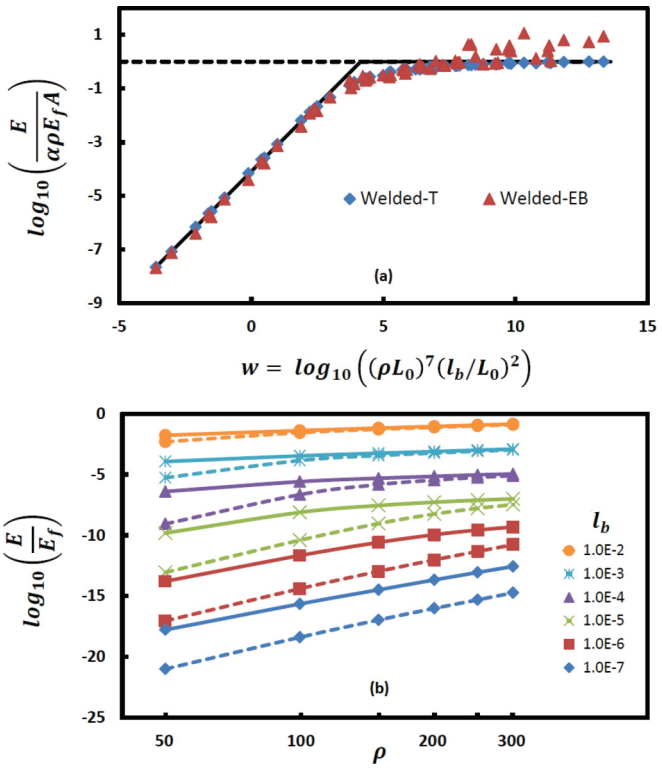

FIG. 1. (Color online) (a) Master curve of the Young's modulus of the network in terms of system parameters (network density, ρ, fiber length, L_0, and parameter l_b) for networks with welded cross-links and in which the fibers are represented with the EB (red triangles) and T (blue diamonds) models. The EB model becomes inaccurate when $w > 7$. The thick lines are added to guide the eye. The inclined continuous line has slope 1. (b) Uncollapsed data from (a) corresponding to the T model and networks with $L_0 = 0.25$ (dashed line) and 1 (solid line).

The curve in Fig. 1(a) has two well-defined regions. At low values of w (small ρ and/or small l_b) the slope is 1, which indicates that Young's modulus E is proportional to ρ^8, L_0^5, and to $(E_f A)l_b^2 = (E_f A)(E_f I/E_f A) = E_f I$ (note the normalization of the vertical axis with ρ, which leads to $E \sim \rho^8$). The axial stiffness of fibers does not appear in the expression of E in this regime. Therefore, the behavior is controlled by the bending deformation mode of the fibers. As w increases, the master curve converges to a horizontal asymptote, which indicates that E is proportional to $E_f A\rho$. In this regime the modulus is independent of the fiber length L_0 and of the bending stiffness of fibers, and the behavior is controlled by the axial deformation mode. A much weaker, linear scaling of E with the density is observed in this regime ($E \sim \rho$). This behavior is similar to that predicted based on the affine deformation assumption, which requires that the local

strain is identical to the global applied strain everywhere in the problem domain. Direct measures of nonaffinity [23,24] also indicate that in the small w range the deformation is strongly nonaffine, while in the limit of large w, the nonaffinity is small. The affine-nonaffine transition described by parameter w can be also controlled by the coordination number, since when z increases above the Maxwell limit ($z_c = 2d$, where d is the dimensionality of the space [10]) the axial mode becomes dominant [13]. However, in 2D, this limit can be approached by increasing L_0 and the effects of increasing L_0 and z cannot be separated. Interesting results have been obtained recently with a special type of 3D models [13,19,20] in which the two parameters could be varied independently. For the regime $z \leqslant z_c$, which is relevant for the present discussion, conclusions qualitatively similar to those obtained for 2D networks resulted: the stiffness vanishes if the fibers have zero bending stiffness, while when $E_f I \neq 0$ a transition from the axial (affine) to the bending (nonaffine) mode is observed as z or/and w decrease.

The strong dependence of the overall modulus on density in the nonaffine range has been studied extensively over the past decade [8,9,11–20]. Numerical studies in Refs. [14,25] led to a smaller exponent, $x = 5.67$, or $E \sim \rho^{6.67}$ for the small w regime of 2D network deformation. Theoretical considerations based on the floppy modes concept led to an exponent close to this value [5]. A similar scaling analysis was presented in Refs. [15,16], leading to the definition of the bending-dominated (nonaffine) and axial-dominated (affine) regimes at small and large w values, respectively. The discussion in these references is in terms of a length parameter, $\lambda = l_c(l_c/l_b)^q$, with L_0/λ being similar to parameter w defined here. $q = 1/3$ gives the prefect collapse for the low-density data, which results in scaling of shear modulus as $G \sim E_f I \rho^9 L_0^6$. The value of exponent q leading to the best collapse at large system densities is $q = 2/5$. Assuming that the modulus is proportional to $(E_f A) l_b^2 \sim E_f I$ in the bending-dominated regime, it is possible to infer from the data in Ref. [15] that the shear modulus scales as $G \sim E_f I \rho^8 L_0^5$, which is identical to our result [Fig. 1(a)]. An effective medium model presented in Ref. [26] suggests a value of $q = 1/4$, smaller than those discussed in Refs. [15,16]. In 3D, the exponents entering parameter w are different. In the affine range the modulus varies as $E_f A \rho$, as in the 2D case, while in the nonaffine range it scales as $G \sim E_f I \rho^3 L_0^2$ [19].

We found that the models used to evaluate E are affected by a strong size effect [17]. Figure 2 shows the variation of the network Young's modulus with the model size, L, for two systems having different values of parameter w, i.e., $w = -3.6$ and 6.4. The density is $\rho = 50$ for both systems, while $l_b = 10^{-7}$ and $l_b = 10^{-2}$ for the systems with $w = -3.6$ and 6.4, respectively. The vertical axis is normalized by the horizontal asymptote of each curve, while the horizontal axis is normalized by the fiber length, L_0 ($L_0 = 0.5$ in both cases). As shown in the figure, the size effect is strong for small w; in order to obtain model size-independent results one needs to consider systems as large as 16 times the fiber length. When w increases, the size effect becomes weak. If models smaller than the threshold insuring model size-independent results are used, data collapse on a master curve may be obtained, but the resulting exponents are

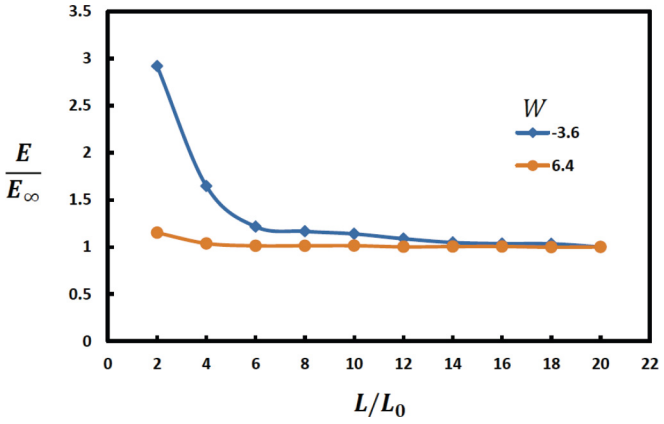

FIG. 2. (Color online) Variation of modulus E with the model size, L, for two values of w. The density $\rho = 50$ in both cases, and $l_b = 10^{-7}$ and 10^{-2} for $w = -3.6$ and 6.4, respectively. The modulus has been normalized with the asymptote value (E_∞) to make the comparison possible. The size effect is more pronounced for the system with nonaffine deformation field ($w = -3.6$), while when the deformation field is affine ($w = 6.4$), the size effect becomes negligible.

smaller than those reported here and the scatter is larger. All data reported in this article are obtained with models free of size effects; for most simulations, especially in the nonaffine range of parameters, the system size was taken $L = 20L_0$.

Let us turn now to the analysis of the effect of model selection on the results discussed above. Figure 1(a) shows data for systems modeled with EB and T beams and with welded cross-links. It is observed that the two models produce similar results in the nonaffine range (w small). As w increases, the EB data do not collapse anymore. This is expected since the EB model is known to become less accurate when the beam aspect ratio decreases, as, for example, in the case of short, stubby network segments. Increasing the bending stiffness (relative to the axial stiffness) results in smaller

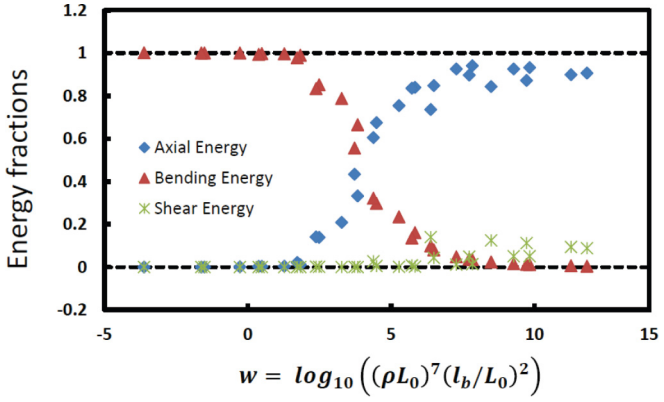

FIG. 3. (Color online) Partition of the strain energy between bending, axial, and shear deformation modes of fibers in systems represented using the Timoshenko model and having welded cross-links, for various values of parameter w. The shear component becomes important for $w > 7$.

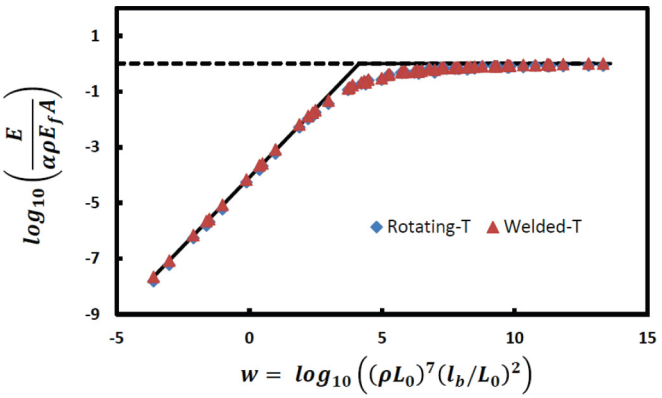

FIG. 4. (Color online) Master curve for the network Young's modulus for networks with welded and rotating cross-links and in which the fibers are represented with the Timoshenko model.

lateral displacements (relative to the axial displacement) for each segment and eventually it causes locking of the lateral displacement. This happens for most short segments resulting in almost rigid subdomains in the network, consequently leading to higher values of the overall stiffness when the EB model is used. This does not happen in the case of T beams since this model has an extra degree of freedom associated with shear deformation. The data indicate that the EB model should be used only for $w < 7$. This is the central result of this work.

To support the statement that the lack of collapse of the EB data in the affine range is due to the failure of the EB model in the respective range of system parameters, let us consider the T model for the beams and evaluate the fraction of energy stored in the axial, bending and shear deformation modes of fibers. This amounts to reporting separately the three terms in Eq. (1). The three energy components are shown in Fig. 3 versus parameter w. In the non-affine range the energy is dominated by the bending component, which is in agreement with the observation stated above that $E \sim E_f I$ in this regime. In the affine range (large w) the energy is partitioned between the axial and shear components, with the bending energy decreasing to zero as w increases. This behavior cannot be captured by the EB model which does not account for shear deformation. The shear component becomes important (approximately 10% of the total energy) for $w > 7$.

Let us compare now systems in which the cross-links are represented by welded and rotating joints. For this purpose, the T model is used for the beams. Figure 4 shows results for the two types of systems and for many networks with different system parameters. The same value of parameter α ($\alpha = 0.38$) was used for all networks considered. It results that the model used for the cross-links is largely inconsequential for the network behavior. The importance of the nature of the cross-links for the mechanical behavior of this type of network was also studied in Refs. [14,27] and a similar conclusion was reported.

The Poisson's ratio was evaluated for all networks considered. This quantity is largely independent of system parameters and takes values close to $\nu = 0.33$ if T beams and rotating joints are used. For the other three modeling options, the Poisson's ratio is ~0.33 if w is small and the deformation is nonaffine. As we have seen, using the EB model in the affine regime (large w) results in a large variability of the Poisson's ratio from realization to realization and a strong dependence on system parameters.

IV. CONCLUSIONS

In this work we have studied the effect of selecting the EB and T models for fibers and welded and rotating representations for the cross-links on the overall elasticity of the network. It was concluded that the EB model should not be used when the system parameters are such that w is larger than 7. In these situations the shear deformation mode of fibers becomes important, which can be captured only by using the T model. The model used for the cross-links is less important, both welded and rotating representations leading to the same scaling and same master curve.

It has been also shown that the strong size effect affecting the network moduli in the nonaffine deformation range may lead to errors in the estimation of the scaling exponents of system stiffness with ρ, L_0, and l_b. Using models large enough to eliminate the size effect, the network modulus in the low density-low l_b range scales as $E \sim E_f I \rho^8 L_0^5$.

[1] K. R. G. Mofrad, *Cytoskeletal Mechanics: Models and Measurements* (Cambridge University Press, Cambridge, 2006).
[2] P. R. Onck, T. Koeman, T. van Dillen, and E. van der Giessen, Phys. Rev. Lett. **95**, 178102 (2005).
[3] D. H. Lee and G. A. Carnaby, Textile Res. J. **62**, 185 (1992).
[4] B. A. DiDonna and T. C. Lubensky, Phys. Rev. E **72**, 066619 (2005).
[5] C. Heussinger, B. Schaefer, and E. Frey, Phys. Rev. E **76**, 031906 (2007).
[6] M. Rigdahl and H. Hollmark, in *Paper Structure and Properties*, edited by J. A. Bristow and P. Koleth (Marcel Dekker, New York, 1986), Ch. 12, p. 241.
[7] R. C. Picu, Soft Matter **7**, 6768 (2011).
[8] C. P. Broedersz, C. Storm, and F. C. MacKintosh, Phys. Rev. Lett. **101**, 118103 (2008).
[9] M. Kellomaki, J. Astrom, and J. Timonen, Phys. Rev. Lett. **77**, 2730 (1996).
[10] J. C. Maxwell, Philos. Mag. **27**, 294 (1864).
[11] M. Wyart, H. Liang, A. Kabla, and L. Mahadevan, Phys. Rev. Lett. **101**, 215501 (2008).
[12] E. M. Huisman and T. C. Lubensky, Phys. Rev. Lett. **106**, 088301 (2011).
[13] C. P. Broedersz, X. Mao, T. C. Lubensky, and F. C. MacKintosh, Nature Phys. **7**, 983 (2011).
[14] J. Wilhelm and E. Frey, Phys. Rev. Lett. **91**, 108103 (2003).
[15] D. A. Head, A. J. Levine, and F. C. MacKintosh, Phys. Rev. E **68**, 061907 (2003).

[16] D. A. Head, A. J. Levine, and F. C. MacKintosh, Phys. Rev. Lett. **91**, 108102 (2003).
[17] A. Shahsavari and R. C. Picu, Int. J. Sol. Struct. (submitted).
[18] E. M. Huisman, T. van Dillen, P. R. Onck, and E. Van der Giessen, Phys. Rev. Lett. **99**, 208103 (2007).
[19] C. P. Broedersz, M. Sheinman, and F. C. MacKintosh, Phys. Rev. Lett. **108**, 078102 (2012).
[20] O. Stenull and T. C. Lubensky, arXiv:1108.4328v1 [cond-mat.soft] (2012).
[21] J. M. Gere and S. P. Timoshenko, *Mechanics of Materials* (PWS Publishers, New York, 1997).
[22] O. Kallmes and H. Corte, Tappi J. **43**, 737 (1960).
[23] J. Liu, G. H. Koenderink, K. E. Kasza, F. C. MacKintosh, and D. A. Weitz, Phys. Rev. Lett. **98**, 198304 (2007).
[24] H. Hatami-Marbini and R. C. Picu, Phys. Rev. E **77**, 062103 (2008).
[25] C. Heussinger and E. Frey, Phys. Rev. Lett. **97**, 105501 (2006).
[26] M. Das, F. C. MacKintosh, and A. J. Levine, Phys. Rev. Lett. **99**, 038101 (2007).
[27] C. Heussinger and E. Frey, Phys. Rev. E **75**, 011917 (2007).